

ScienceDirect



IFAC PapersOnLine 56-3 (2023) 301-306

Safe Model-Based Multivariable Control of Peritoneal Perfusion

Yejin Moon* Behzad KadkhodaeiElyaderani*
Joshua Leibowitz** Parham Rezaei* Eman M. Abdelazim*
Morcos Awad** Stephen Stachnik** Shelby Stewart***
Joseph S. Friedberg**** Jin-Oh Hahn† Hosam K. Fathy†

* Mechanical Eng. Ph.D. student, Univ. of Maryland, College Park.

** Resident physician, University of Maryland School of Medicine.

*** Thoracic surgeon, University of Maryland School of Medicine.

**** Thoracic Surgeon, Temple University.

† Prof. of Mechanical Eng., Univ. of Maryland, College Park (address all correspondence to H. K. Fathy, hfathy@umd.edu).

Abstract: This paper examines the control of abdominal perfusion during medical interventions. The goal is to avoid safety risks such as excessive retained fluid volume, tissue damage/trauma, and intra-abdominal hypertension. The paper presents a perfusion system with peristaltic pumps dictating fluid inflow/outflow rates, and uses model-based control to avoid multiple safety risks simultaneously. Specifically, the paper: (i) introduces a discharge efficiency metric reflecting the risk of tissue trauma and/or outflow cavitation; (ii) identifies a dynamic model of discharge efficiency from animal test data; and, (iii) develops a safe perfusion control algorithm based on this model. The algorithm receives three user inputs: a desired inflow rate, a desired perfused volume, and a safety bound on discharge efficiency. The algorithm minimizes the deviation of the commanded inflow/outflow rates from a nonlinear model reference controller, subject to a barrier constraint on discharge efficiency. This furnishes a switching control structure providing convergence to the desired perfusion settings in the absence of outflow occlusion, and operating safely when outflow is occluded, as shown in simulation-based validation studies.

Copyright © 2023 The Authors. This is an open access article under the CC BY-NC-ND license (https://creativecommons.org/licenses/by-nc-nd/4.0/)

Keywords: Safe model reference control; barrier functions; biomedical devices; perfusion.

1. INTRODUCTION

This paper introduces an algorithm for controlling peritoneal perfusion in a manner that avoids multiple potential safety risks. Peritoneal perfusion is the circulation or dwelling of a fluid through a patient's or lab animal's peritoneal (abdominal) cavity. This typically involves the insertion of one or more cannulas into the abdominal cavity to perfuse/drain fluid. This enables diffusion-based transport between the fluid and the blood vessels.

Peritoneal perfusion is used for removing toxins from the bloodstream during peritoneal dialysis, allowing the abdomen to serve as a "third kidney". Another application is hyperthermic chemotherapy, where a chemotherapy drug is circulated through the peritoneal cavity for a short period of time to treat abdominal cancer. Potential future applications include the peritoneal perfusion of oxygen carriers, such as perfluorocarbons (PFCs). PFCs are clear, dense liquids that have high oxygen and carbon dioxide solubilities, and have been examined as blood substitutes (Castro and Briceno (2010); Biro et al. (1987)). This paper is partly motivated by the potential of oxygenated PFC perfusion to serve as a "third lung" by providing life support for patients with ailments such as COVID-19 and acute respiratory distress syndrome (Carr et al. (2006)).

Fig. 1 presents a schematic of a "third lung" setup developed and utilized by the authors in 13 experiments on

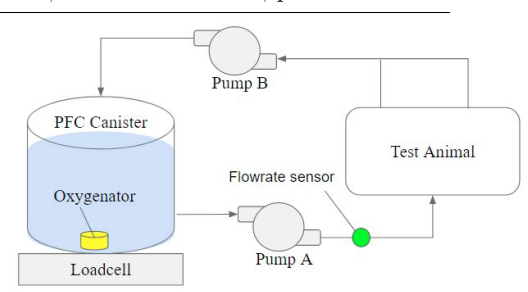


Fig. 1. Animal Experiment Setup

Yorkshire swine to date. This setup stores PFC in a canister equipped with a bubble oxygenator. Two reversible peristaltic pumps are used for PFC delivery to the animal (Pump A) and PFC drainage (Pump B).

Peritoneal perfusion comes with at least two safety risks. The first risk arises when the intra-abdominal volume (IAV), i.e., the perfusate volume retained in the abdomen, is too high. The effectiveness of peritoneal perfusion depends on IAV, creating a need to optimize perfusate volume for each patient (Durand et al. (2000); Fischbach et al. (2005)). However, a high IAV can result in excessive intra-abdominal pressure (IAP). An IAP above 12mmHg can cause intra-abdominal hypertension (IAH) (Kirkpatrick et al. (2013)). If IAH persists for a significant amount of

time or if IAP exceeds 20mmHg, abdominal compartment syndrome can occur. This is a life-threatening condition that can cause organ failures in the cardiovascular, renal, digestive, and respiratory systems (Kirkpatrick et al. (2013); Blaser et al. (2015); Sugrue (2005)). The second risk is associated with the suction pressure used for fluid drainage. Suction devices are widely used in medicine to remove/collect liquids, solids, and gases from the body (Shannon and Goldsmith (2009)), with greater negative pressures creating greater drainage flowrates (Rosen and Hillard (1960)). However, excessive suction pressures have the potential to cause cavitation, tissue trauma, and serosal damage (Rosen and Hillard (1960)). Serosal damage can, in turn, cause bleeding, anemia, and the formation of scar tissue (Patricia Carroll (2010)).

The literature examines the dynamic relationship between IAP and IAV in applications such as abdominal paracentesis, laparoscopic pneumoperitoneum, and dialysis (e.g., Chiumello et al. (2007); Yoshino et al. (2012); Zaleski et al. (2022)). The literature also presents various ways to measure/monitor IAP (Kirkpatrick et al. (2013); Malbrain et al. (2016)), plus guidelines for manually performing safe suctioning in different applications, such as endotracheal suctioning, liposuction, and pneumothorax treatment (Rosen and Hillard (1960); Brooks et al. (2001); Glass and Grap (1995); Henry et al. (2003)). These guidelines commonly recommend using low suction pressure to avoid bleeding and tissue damage. However, there are nontrivial tradeoffs between different perfusion/safety objectives. For instance, decreasing suction pressure can reduce the risk of serosal damage, at the expense of curtailing drainage and elevating the risk of excessive IAV/IAP. This creates a need for a perfusion controller that simultaneously addresses multiple tracking/safety objectives.

This paper addresses the above need by adding three novel contributions to the literature. First, the paper uses least squares estimation with exponential forgetting (Section 3) to estimate perfusate "drainage efficiency" (i.e., the ratio of the true drainage rate to the commanded rate). Poor drainage efficiency is indicative of excessive suction, tissue trauma/occlusion at the drainage catheter, serosal damage, and/or fluid cavitation. Second, the paper uses data from an animal experiment (described in Section 2) to (i) validate the ability of the drainage efficiency estimator to detect deliberate outflow occlusion and (ii) identify a state-space model of drainage efficiency dynamics (Section 3). Finally, the paper presents a multivariable algorithm that uses nonlinear model reference control to track the desired perfusion flowrate and IAV, subject to a safety barrier penalty for low drainage efficiencies (Section 4). A simulation study shows that this controller provides exponential convergence to the desired perfusion conditions in the absence of outflow occlusion, and operates safely when outflow is occluded (Sections 4-5).

2. PERFUSION EXPERIMENT

The paper's modeling, estimation, and control efforts are based on a flow occlusion experiment performed using the setup in Fig. 1, and described below. An adult male Yorkshire swine with an approximate mass of 45kg was anesthetized, then its abdomen was intubated for perfusion with an oxygenated cis-\trans- perfluorodecalin mix.

Three 12mm diameter venous cannulas terminating in foam-covered diffusers were used for perfusion. One cannula supplied oxygenated PFC from Pump A to the animal's upper abdomen in the supine position. Two additional cannulas provided drainage from each lower quadrant of the abdomen. These cannulas were connected to Pump B through a Y-junction. The setup oxygenated the PFC and controlled its temperature, as described in an earlier article by the authors (Doosthosseini et al. (2021)). Additionally, a scale (or load cell) under the PFC canister measured the amount of PFC left in the setup's canister. A PID controller enabled Pump A to accurately track the desired flowrate of PFC into the animal, based on feedback measurements of this flowrate from a fluid flow sensor.

The ultimate goal of this paper is to develop a perfusion controller that tracks a user-specified perfusion flowrate and IAV while avoiding unsafe (i.e., low) drainage efficiencies. This goal assumes that the perfusionist (i.e., setup operator) selects the target IAV to provide a reasonable tradeoff between perfusion effectiveness and safety. Towards this goal, the investigators conducted an experiment where an initial volume of PFC was provided to a laboratory animal and allowed to dwell prior to 1160 seconds of PFC circulation. Two 60-second occlusion episodes were induced during circulation by pinching one of the drainage cannulas (at the 440-second mark), then pinching both drainage cannulas simultaneously (at the 660-second mark). The remainder of this paper uses the results of this experiment to develop: (i) an occlusion detection algorithm, (ii) a fluid drainage efficiency model, and (iii) a safe perfusion controller. Throughout this work, poor drainage efficiency is employed as an occlusion metric.

3. DRAINAGE EFFICIENCY ESTIMATION AND MODELING

Let drainage efficiency, θ , be the ratio of the true fluid drainage flowrate, $u_{2,true}(t)$, to the flowrate command sent to Pump B, $u_2(t)$. Stated mathematically, $\theta = u_{2,true}/u_2$. Drainage efficiency can be computed directly if the true drainage flowrate is measured. However, given the cost of high-quality flowrate sensors, this paper examines the problem of estimating drainage efficiency from load cellbased estimates of the volume, $x_1(t)$, of fluid inside the perfusion canister. Towards this goal, note that the perfused fluid is incompressible, and that it is supplied to the animal using a peristaltic (i.e., positive displacement) pump namely, Pump A. Therefore, it is reasonable to assume that Pump A accurately provides the desired fluid flowrate into the animal, even in open-loop mode. In contrast, when the outflow cannula is occluded, fluid cavitation typically occurs upstream of the drainage pump (i.e., Pump B), resulting in a discrepancy between the commanded and actual drainage flowrates. Denoting the commanded Pump A flowrate by $u_1(t)$ hence leads to the following state equation for the volume of PFC in the setup's canister:

$$\dot{x}_1 = \theta u_2 - u_1 \tag{1}$$

The first contribution of this paper is to develop an estimator for fluid drainage efficiency, θ . The estimator solves the following continuous-time least squares problem:

$$\min_{\theta} \int_{-\infty}^{t} (\dot{x}_1(\tau) + u_1(\tau) - \theta u_2(\tau))^2 e^{-\lambda(t-\tau)} d\tau \qquad (2)$$

where $\lambda=0.02sec^{-1}$ is a forgetting factor, reflecting the assumption that changes in drainage efficiency take place over durations larger than roughly 50 seconds. The analytic solution to this regression problem is:

$$\theta = \frac{\int_{-\infty}^{t} (\dot{x}_1(\tau) + u_1(\tau)) u_2(\tau) e^{-\lambda(t-\tau)} d\tau}{\int_{-\infty}^{t} u_2^2(\tau) e^{-\lambda(t-\tau)} d\tau}$$
(3)

The above algorithm was implemented in Simulink with an integration step size of 0.01 sec. This furnished a drainage efficiency estimator, useful in its own right as a tool for monitoring perfusion safety. Initial conditions of $19 \ L^2 sec^{-1}$ and $20 \ L^2 sec^{-1}$ were used for the estimator's numerator and denominator integrals, respectively, at t=0, corresponding to an assumed initial efficiency of $95 \ \%$.

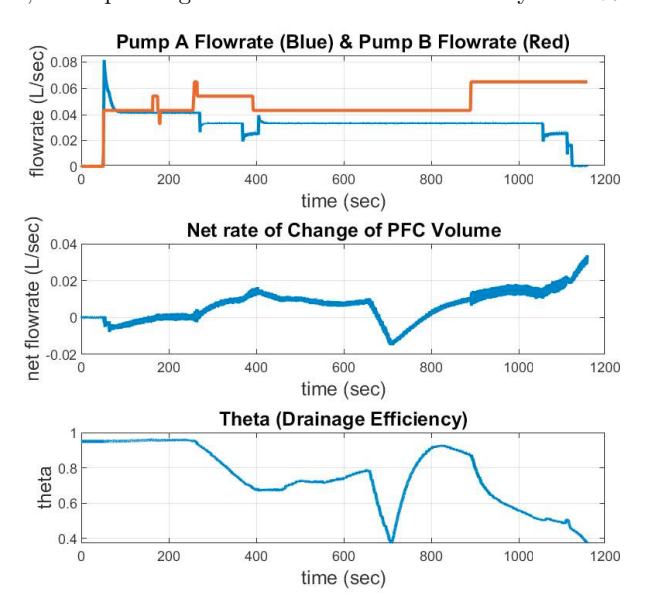


Fig. 2. Pump A & B flowrates, rate of change of PFC volume in the canister, and drainage efficiency

Fig. 2 summarizes the results of this drainage efficiency estimation effort. The top plot shows the rate of PFC volume change in the setup's canister over time, measured using the load cell, in L/sec. The bottom plot presents the estimated θ , or flowrate efficiency, during circulation. Five distinct phases are visible in Fig. 2. First, between roughly 0-250 seconds, PFC is circulated at roughly equal inflow/outflow rates. The net volume of PFC in the canister does not change significantly, and the estimated drainage efficiency is high. Second, between roughly 250-400 seconds, a larger command is given to Pump B versus Pump A, corresponding to a desire to drain PFC from the animal. The volume of PFC in the canister increases, but drainage efficiency experiences a significant drop. Third, between roughly 400-660 seconds, flowrate commands are adjusted to drain the animal more gradually. The volume of PFC in the canister continues to increase, but drainage efficiency recovers slowly. Interestingly, the pinching of one of the outflow cannulas at roughly 440 seconds does not have a visible effect on the plots, which makes sense given that only one of the outflow cannulas was pinched. Fourth, at around 660- second mark, both outflow cannulas are artificially occluded, resulting in a dramatic temporary

decline in drainage efficiency. Finally, after the 800— second mark, flowrate commands are adjusted to drain the animal aggressively. Fluid accumulates in the canister, but drainage efficiency declines significantly.

The above results are very encouraging for two reasons. First, they clearly show the success of the drainage efficiency estimator in detecting complete occlusion of fluid outflow around the 660- second mark. Second, it makes intuitive sense for outflow occlusion to be more prevalent during time periods when Pump B is operated more aggressively than Pump A, for the purpose of providing net fluid drainage. This is consistent with visual observations during the experiment, where outflow cavitation occurred more frequently during those periods. Motivated by this success, the paper's second contribution is to fit a simple data-driven state-space model for drainage efficiency:

$$\dot{x}_2 = \alpha_1 u_1 + \alpha_2 u_2 + \alpha_3 x_2 + \alpha_4, \quad \theta = \frac{e^{x_2}}{1 + e^{x_2}}$$
 (4)

where θ is related to a data-driven state variable, x_2 , through a sigmoidal function that bounds θ between 0 and 1. The dynamics of the occlusion-related state variable, x_2 , are governed by a simple linear data-driven state equation with unknown constant parameters α_1 , α_2 , α_3 , and α_4 . These parameters were obtained by fitting Eq. 4 to animal test data using MATLAB's particle swarm optimization algorithm. The optimization objective was to minimize the summation of the squared differences between the θ curve from Fig. 2 and the predicted θ from Eq. 4. To minimize the effect of any unmodeled dynamics (e.g., pinching of the cannulas), only the last 300-second portion of the dataset was used to fit the model.

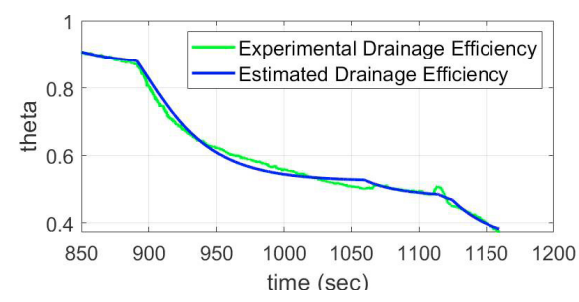


Fig. 3. Drainage efficiencies from Fig. 2 and Eq. 4

Fig. 3 compares the experimental drainage efficiency from Fig. 2 to the estimated efficiency from Eq. 4. Here, the parameter estimates are $\alpha_1 = 0.5870$, $\alpha_2 = -1.6581$, $\alpha_3 = -0.0248$, and $\alpha_4 = 0.0900$. As shown in the graph, the estimated efficiency follows the experimental results fairly well. Moreover, the signs and relative values of the estimated parameters make intuitive sense. Specifically, the fact that $\alpha_3 < 0$ furnishes a stable model. Furthermore, the fact that $\alpha_1 > 0$ implies that increasing commanded fluid inflow has the potential to improve drainage efficiency by pushing fluid through the abdomen. This makes intuitive sense for two reasons. First, increasing the fluid inflow rate has the potential to raise intra-abdominal pressure to promote drainage. Second, a larger PFC inflow rate can reduce occlusion from the surface of the bowels by enabling the dense PFC to push the bowels upwards towards the surface of the ventral abdominal wall, away from the dorsally located drainage cannulas. In contrast to α_1 , the fact that $\alpha_2<0$ suggests that increasing Pump B flowrate can decrease the drainage efficiency. This agrees with the reports from the literature and the observations from our animal experiments: the greater the applied suction command, the greater the risk of occlusion of the drainage catheter. Finally, the values of α_3 and α_4 imply that when both inputs are zero (i.e., no perfusion or drainage flowrate), θ will be equal to 0.9743 in steady state. This means that there would be almost no steady-state occlusion when both pumps are turned off, which makes intuitive sense. As a result, the full state-space model becomes:

$$\dot{x}_1 = \theta u_2 - u_1, \quad \dot{x}_2 = \alpha_1 u_1 + \alpha_2 u_2 + \alpha_3 x_2 + \alpha_4 \tag{5}$$

Again, x_1 is the PFC volume in the canister, x_2 is drainage efficiency, and $\theta = \frac{e^{x_2}}{1+e^{x_2}}$. This model serves as the plant model for the design of the safety controller, as described in the next section.

4. PERFUSION SAFETY CONTROLLER

To prevent occlusion while performing effective perfusion, a controller must maintain the desired fluid volume in the PFC canister, track the user-specified PFC flowrate, and ensure that $\theta=x_2$ stays above a user-specified safe minimum value. To satisfy these objectives, this section begins by constructing the following barrier function:

$$f_b(x_2, x_{2,min}) = x_2 - x_{2,min} (6)$$

where $x_{2,min}$ is a safe lower bound on x_2 . The monotonic/sigmoidal relationship between x_2 and drainage efficiency implies that $x_{2,min} = \ln \frac{\theta_{min}}{1-\theta_{min}}$ for any desired minimum drainage efficiency, θ_{min} . For perfusion safety, the barrier function f_b must always be positive. Moreover, it should recover to a positive value if it starts from a negative initial condition. This can be achieved by imposing the following constraint on the barrier function's time derivative:

$$\frac{\mathrm{d}f_b}{dt} \ge -\lambda_2 f_b \tag{7}$$

where the constant λ_2 dictates the rate of recovery of the barrier function. Substituting Eq. 6 into Eq. 7 furnishes the following constraint:

$$\dot{x}_2 \ge -\lambda_2(x_2 - x_{2,min}) = \lambda_2(x_{2,min} - x_2)$$
 (8)

Next, substituting \dot{x}_2 from Eq. 5 into Eq. 8 gives:

$$\alpha_1 u_1 + \alpha_2 u_2 + \alpha_3 x_2 + \alpha_4 \ge \lambda_2 (x_{2,min} - x_2) \tag{9}$$

The goal of this perfusion controller is to track a user-specified perfusion flowrate, $u_{1,des}$, plus a user-specified volume of PFC in the setup's canister, $x_{1,des}$, subject to the above safety constraint. Specifically, the controller solves this optimization problem at every instant in time:

$$\min_{u_1, u_2} (u_1 - u_{1,des})^2 \quad sub. \ to:$$

$$\alpha_1 u_1 + \alpha_2 u_2 + \alpha_3 x_2 + \alpha_4 \ge \lambda_2 (x_{2,min} - x_2)$$

$$\dot{x}_1 = \frac{e^{x_2}}{1 + e^{x_2}} u_2 - u_1 = \lambda_1 (x_{1,des} - x_1)$$

$$\dot{x}_2 = \alpha_1 u_1 + \alpha_2 u_2 + \alpha_3 x_2 + \alpha_4$$
(10)

In the above problem, the objective is to minimize the difference between the user-specified ideal perfusion flowrate, $u_{1,des}$, and the true Pump A flowrate, u_1 . Achieving the ideal flowrate exactly is not always feasible, given the potential need for ensuring safety through flowrate curtailment. Optimization is performed subject to the safety

barrier function as an inequality constraint. This guarantees perfusion safety in the sense that if drainage efficiency is safe initially, it remains safe subsequently. Moreover, optimization is performed subject to an equality constraint on the time derivative of the volume of PFC in the setup's canister, \dot{x}_1 . Here, $\lambda_1(x_{1,des}-x_1)$ is set to be the reference model for \dot{x}_1 . This equality constraint guarantees the exponential convergence of this volume, x_1 , to its desired value, $x_{1,des}$, at a rate governed by the design constant, λ_1 . By construction, therefore, this optimization problem ensures exponential convergence to the desired volume of PFC in the perfusion canister (or IAV), regardless of whether the drainage efficiency safety constraint is active or inactive.

The solution to the above optimization problem is a switching control policy. When the perfusion safety barrier function is inactive, the controller follows a simple model reference control policy, where $u_1 = u_{1,des}$ and u_2 is obtained by solving the following equality constraint:

$$\dot{x}_1 = \frac{e^{x_2}}{1 + e^{x_2}} u_2 - u_{1,des} = \lambda_1 (x_{1,des} - x_1)
\Rightarrow u_2 = \frac{\lambda_1 (x_{1,des} - x_1) + u_{1,des}}{\frac{e^{x_2}}{1 + e^{x_2}}}$$
(11)

In contrast, when the drainage efficiency safety barrier is active, the control inputs are governed by:

$$\begin{bmatrix} -1 & \theta \\ \alpha_1 & \alpha_2 \end{bmatrix} \begin{bmatrix} u_1 \\ u_2 \end{bmatrix} = \begin{bmatrix} \lambda_1 (x_{1,des} - x_1) \\ \lambda_2 (x_{2,min} - x_2) - \alpha_3 x_2 - \alpha_4 \end{bmatrix}$$
(12)

To summarize, the basic idea behind the proposed controller can be explained as follows. The controller assumes that the PFC volume in the canister is measured. The desired PFC volume, the desired Pump A flowrate, and minimum safe drainage efficiency, θ , are commanded by the user. At every instant in time, the controller assumes that $u_1 = u_{1,des}$, employs Eq. 11 to solve for u_2 , and checks if the resulting unconstrained control policy satisfies the safety barrier constraint in Eq. 9. If the safety barrier constraint is satisfied, the unconstrained values of u_1 and u_2 are implemented. But if the above values of u_1 and u_2 violate the safety barrier constraint, then the controller

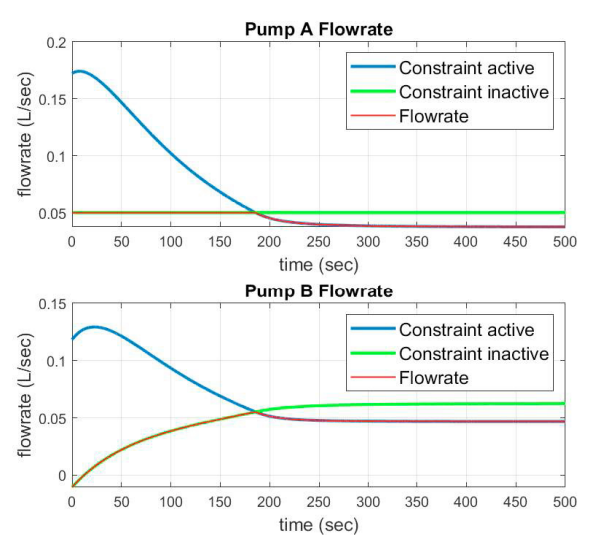


Fig. 4. Safety-Controlled Pump Flowrates - Scenario I

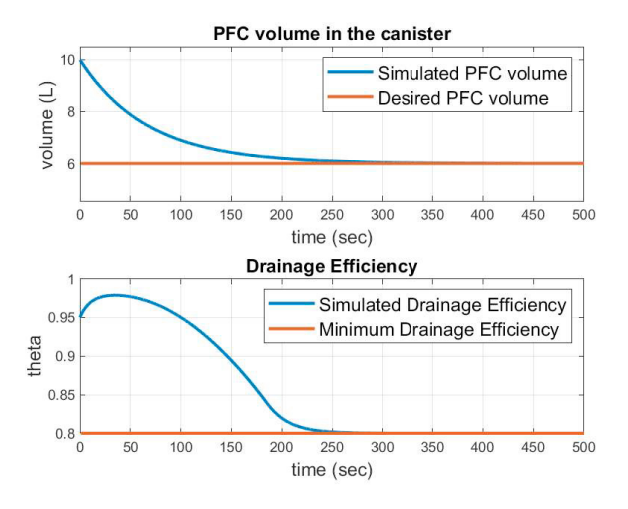


Fig. 5. Safety Control Results - Scenario I

uses Eq. 12 to compute the constrained values of u_1 and u_2 , then commands these values to the peristaltic pumps.

To evaluate the performance of the controller, two scenarios with different initial θ conditions are simulated for 500 seconds. The initial condition for PFC volume in the canister is set to be 10 L, and the desired value of this volume is chosen to be 6 L. This is equivalent to providing 4 L of PFC to the animal. The design constants, λ_1 and λ_2 , are set to be $0.015 \ sec^{-1}$ and $0.05 \ sec^{-1}$, respectively. The value of λ_1 corresponds to a time constant of 66.7 seconds for converging to the desired perfused fluid volume, and the value of λ_2 corresponds to a time constant of 20 seconds for converging to safe perfusion conditions. The desired Pump A flowrate is chosen as 0.05 L/sec, a typical value used during animal perfusion experiments to date. Lastly, the minimum safety θ is set to 0.8, considering that θ dropped to 0.7 when one of the outflow tubes was occluded in Fig. 2. The controller is simulated twice with two different initial θ values of 0.95 (little to no initial occlusion) and 0.1 (a severe initial occlusion).

4.1 Scenario I - Low Initial Occlusion

In this scenario, the initial condition for drainage efficiency is set to 0.95, with Fig. 4 and Fig. 5 showing the associated simulated performance of the safety controller. Fig. 4 shows the flowrates commanded to the two peristaltic pumps versus time, highlighting the periods of time when these flowrates coincide with unconstrained vs. constrained control. Fig. 5 shows the volume of PFC in the perfusion canister and drainage efficiency versus time.

Fig. 4 shows that the controller's simulated performance achieves all control design objectives. Initially, the drainage efficiency is above its minimum value, making both pumps implement the unconstrained optimal flowrates. Specifically, Pump A implements the desired perfusion flowrate exactly. Moreover, Pump B briefly implements a negative flowrate: an interesting result that is physically feasible and corresponds to the goal of delivering PFC to the animal faster. These flowrates cause drainage efficiency to improve and the PFC volume in the canister to decrease. However, after 25- second mark, the drainage efficiency gradually decreases due to the

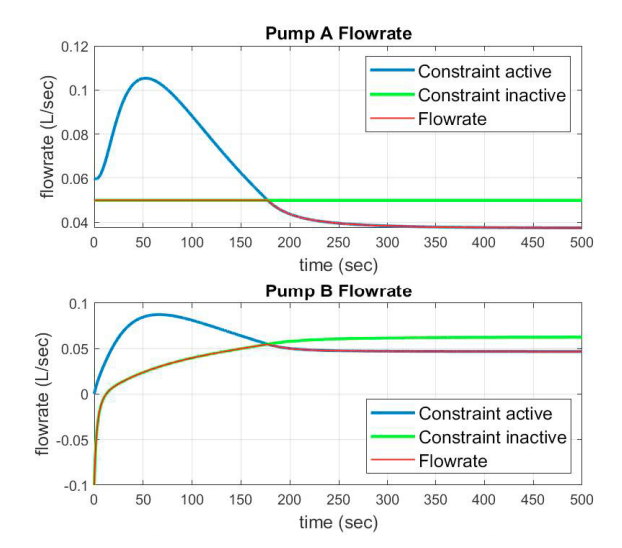


Fig. 6. Safety-Controlled Pump Flowrates - Scenario II

growing Pump B flowrate. The pumps continue following the unconstrained signals until the PFC volume in the canister and the drainage efficiency become closer to their desired/minimum values. At around the 180- second mark, both pumps switch to the constrained optimal flowrates. Yet, the implementation of a safety barrier constraint ensures that drainage efficiency never drops below 80%. Moreover, even as the controller switches from unconstrained to constrained operation, the volume of PFC in the setup converges to its target value, as desired.

4.2 Scenario II - Severe Initial Occlusion

In this scenario, drainage efficiency is initialized to 0.1, reflecting severe initial occlusion. Fig. 6 shows the pump flowrates from this simulation. Initially, the two pumps follow the unconstrained control signals. This reflects the fact that, even though drainage efficiency starts below 0.8, unconstrained control satisfies the safety barrier constraint and brings this efficiency back above its safe minimum value. Also, similar to the previous scenario, Pump B starts at a negative initial flowrate which improves the

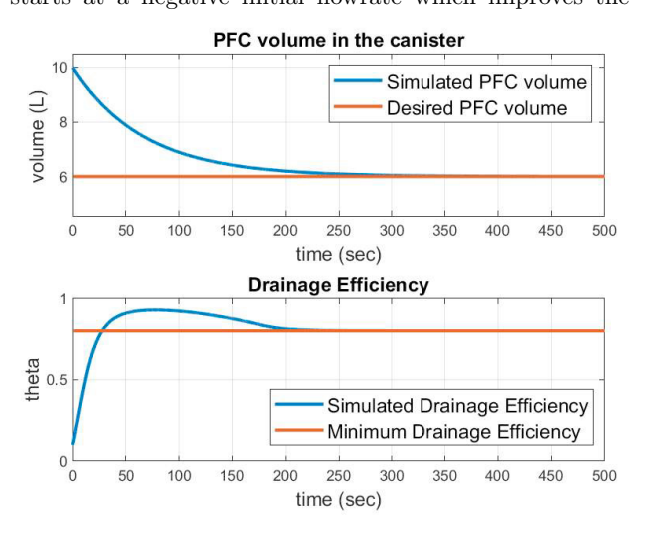


Fig. 7. Safety Control Results - Scenario II

drainage efficiency and achieves the desired PFC volume in the canister rapidly. Over time, the volume of PFC in the perfusion canister reaches its desired target exponentially, as shown in Fig. 7. The associated increase in Pump B flowrate causes drainage efficiency to decline, approaching its minimum safe value. This triggers the pumps to switch to the constrained control signals around the 180- second mark. During the rest of the simulation, both the PFC volume in the canister and the drainage efficiency stay at the desired/safe values, highlighting the success of the switching controller in performing safe perfusion.

5. DISCUSSION AND CONCLUSION

This paper makes three contributions to the literature. The first contribution is an algorithm for estimating drainage efficiency in peritoneal perfusion applications. This algorithm is valuable in its own right as an online perfusion safety monitoring tool, and is successful in detecting the deliberate occlusion of perfusion outflow in an animal experiment. The second contribution is a datadriven model of drainage efficiency dynamics, parameterized using animal test data. This model can serve as a foundation for safe perfusion system modeling, design, and control. The third contribution is a model-based perfusion safety controller that simultaneously adjusts multiple perfusion pump flowrates in pursuit of multiple perfusion safety and tracking objectives. To the best of the authors' knowledge, this controller represents the first application of multivariable safety control to perfusion problems. The controller's performance is validated for two distinct simulation scenarios, and meets the control design requirements in both scenarios.

One interesting observation regarding the controller is its tendency to improve drainage, or outflow, from the abdomen by pushing fluid through the inflow line at a larger volumetric flowrate, in addition to curtailing the fluid outflow command. It is important to validate this strategy and the underlying control policy against more animal test data, and ultimately in the laboratory. Moreover, the controller's implementation can potentially benefit from the online estimation of drainage efficiency model parameters as part of an adaptive control structure. Both of these topics represent potentially valuable future research directions.

REFERENCES

- Biro, G.P., Blais, P., and Rosen, A.L. (1987). Perfluorocarbon blood substitutes. *Critical reviews in oncology/hematology*, 6(4), 311–374.
- Blaser, A.R., Björck, M., De Keulenaer, B., and Regli, A. (2015). Abdominal compliance: a bench-to-bedside review. Journal of Trauma and Acute Care Surgery, 78(5), 1044–1053.
- Brooks, D., Anderson, C.M., Carter, M.A., Downes, L.A., Keenan, S.P., Kelsey, C.J., and Lacy, J.B. (2001). Clinical practice guideline for suctioning the airway of the intubated and non-intubated patient. *Canadian Respiratory Journal*, 8(3), 163–181.
- Carr, S.R., Cantor, J.P., Rao, A.S., Lakshman, T.V., Collins, J.E., and Friedberg, J.S. (2006). Peritoneal perfusion with oxygenated perfluorocarbon augments systemic oxygenation. *Chest*, 130(2), 402–411.

- Castro, C.I. and Briceno, J.C. (2010). Perfluorocarbonbased oxygen carriers: review of products and trials. Artificial organs, 34(8), 622–634.
- Chiumello, D., Tallarini, F., Chierichetti, M., Polli, F., Bassi, G.L., Motta, G., Azzari, S., Carsenzola, C., and Gattinoni, L. (2007). The effect of different volumes and temperatures of saline on the bladder pressure measurement in critically ill patients. *Critical care*, 11(4), 1–7.
- Doosthosseini, M., Aroom, K.R., Aroom, M., Culligan, M., Naselsky, W., Thamire, C., Haslach Jr, H.W., Roller, S.A., Hughen, J.R., Friedberg, J.S., et al. (2021). Monitoring and control system development and experimental validation for a novel extrapulmonary respiratory support setup. arXiv preprint arXiv:2107.02902.
- Durand, P.Y., Balteau, P., Chanliau, J., and Kessler, M. (2000). Optimization of fill volumes in automated peritoneal dialysis. *Peritoneal dialysis international*, 20(2_suppl), 83–88.
- Fischbach, M., Dheu, C., Helms, P., Terzic, J., Michallat, A.C., Laugel, V., Wolff-Danner, S., and Haraldsson, B. (2005). The influence of peritoneal surface area on dialysis adequacy. *Peritoneal dialysis international*, 25(3_suppl), 137–140.
- Glass, C.A. and Grap, M.J. (1995). Ten tips for safer suctioning. *The American journal of nursing*, 95(5), 51–53.
- Henry, M., Arnold, T., and Harvey, J. (2003). Bts guidelines for the management of spontaneous pneumothorax. *Thorax*, 58(Suppl 2), ii39.
- Kirkpatrick, A.W., Roberts, D.J., De Waele, J., Jaeschke, R., Malbrain, M.L., De Keulenaer, B., Duchesne, J., Bjorck, M., Leppaniemi, A., Ejike, J.C., et al. (2013). Intra-abdominal hypertension and the abdominal compartment syndrome: updated consensus definitions and clinical practice guidelines from the world society of the abdominal compartment syndrome. *Intensive care medicine*, 39, 1190–1206.
- Malbrain, M.L., Peeters, Y., and Wise, R. (2016). The neglected role of abdominal compliance in organ-organ interactions. *Critical Care*, 20(1), 1–10.
- Patricia Carroll, R. (2010). Enhancing the safety of medical suction through innovative technology. *Canadian Journal of Respiratory Therapy*, 46(2), 47.
- Rosen, M. and Hillard, E. (1960). The use of suction in clinical medicine. *British Journal of Anaesthesia*, 32(10), 486–504.
- Shannon, A. and Goldsmith, A. (2009). Suction devices. Anaesthesia & Intensive Care Medicine, 10(10), 468–470.
- Sugrue, M. (2005). Abdominal compartment syndrome. Current opinion in critical care, 11(4), 333–338.
- Yoshino, O., Quail, A., Oldmeadow, C., and Balogh, Z.J. (2012). The interpretation of intra-abdominal pressures from animal models: the rabbit to human example. *Injury*, 43(2), 169–173.
- Zaleski, N., Moon, Y., Doosthosseini, M., Hopkins, G., Aroom, K., Aroom, M., Naselsky, W., Culligan, M.J., Leibowitz, J., Shah, A., et al. (2022). Modeling and experimental identification of peritoneal cavity pressure dynamics during oxygenated perfluorocarbon perfusion. In 2022 European Control Conference (ECC), 297–302. IEEE.